

Comparative Studies of Kinetics of Nanocomposite Poly-*o*-toluidine Zr(IV) Phosphate and Fibrous Nylon-6,6 Sn(IV) Phosphate Cation Exchange Materials

ASIF ALI KHAN* and TABASSUM AKHTAR

Analytical Research Laboratory, Department of Applied Chemistry,
Faculty of Engineering and Technology, Aligarh Muslim University, Aligarh-202002, India
asifkhan42003@yahoo.com

Received 22 February 2013 / Accepted 19 March 2013

Abstract: An organic-inorganic composite, poly-*o*-toluidine Zr(IV) phosphate and nylon-6,6 Sn(IV) phosphate was chemically synthesized by mixing ortho-toluidine and nylon-6,6 into the gel of Zr(IV) phosphate and Sn(IV) phosphate in different mixing volume ratios. The particle diffusion mechanism is confirmed by the linear τ (dimensionless time parameter) vs. t (time) plots. This study revealed the exchange process controlled by the diffusion within the exchanger particles. Some physical parameters like self-diffusion coefficient (D_0), activation energy (E_a) and entropy of activation (ΔS°) have been evaluated under conditions favoring a particle diffusion-controlled mechanism.

Keywords: Cation exchangers, Poly-*o*-toluidine Zr(IV)phosphate, Nylon-6,6 Sn(IV) Phosphate, Ion-exchange Kinetics

Introduction

Ion exchange separations are essentials parts of different techniques and technologies. Various applications of ion exchangers can be found in pharmaceuticals and medicine¹⁻³, recuperation of metals⁴, biotechnology⁵ catalysis⁶, food production⁷⁻¹², recycling of industrial waste¹³⁻¹⁴, microelectronics, nuclear industry¹⁵⁻¹⁷, potable water preparation¹⁸⁻²⁰ and many other areas. Ion exchange is a powerful tool in chemical analysis and scientific research. The course can be useful for students studying Chemistry, Chemical Technology and materials Chemistry as well as for industrial specialists working with ion exchange or separation processes²¹. Ion exchange is also widely used in the food & beverage, hydrometallurgical, metals finishing, chemical & petrochemical, pharmaceutical, sugar & sweeteners, ground & potable water, nuclear, softening & industrial water, semiconductor, power and a host of other industries. The poly-*o*-toluidine Zr(IV) phosphate nanocomposite and fibrous nylon-6,6 Sn(IV) phosphate cation-exchanger was selective for Hg(II) having good cation-exchange capacity. Various ion-exchange studies of the composites are carried out. Separation of Hg(II) from other heavy metal ions have been done by this exchangers.

Poly-*o*-toluidine Zr(IV) phosphate, a nano-composite and nylon-6,6 Sn(IV) phosphate, a fibrous cation-exchange materials have shown excellent ion-exchange properties. The mechanism of ion exchange can be explained taking into account of ion-exchange equilibrium with respect to time and the phenomenon of ion-exchange is considered as diffusion of ion through particles of the exchanger and its adherent film. With the help of experimental data and mathematical computations some physical parameters like self diffusion co-efficient (D_0), energy of activation (E_a) and entropy of activation (ΔS^0) are obtained.

Experimental

The main reagents used were obtained from CDH, Loba Chemie, E-Merck and Qualigens (India Ltd., used as received). All other reagents and chemicals were of analytical grade. Following instruments were used during present research work: digital pH-meter (Elico Li-10, India); a digital potentiometer (Equiptronics EQ 609, India); an electronic balance (digital, Sartorius-210S, Japan) and an automatic temperature controlled water bath incubator shaker - Elcon (India) were used.

Preparation of organic-inorganic composite cation exchanger

Preparation of poly-o-toluidine Zr(IV) phosphate

The composite cation-exchanger was prepared by the sol-gel mixing of poly-*o*-toluidine, an organic polymer, into the inorganic precipitate of Zr(IV) phosphate. In this process, when the gels of poly-*o*-toluidine were added to the white inorganic precipitate of Zr(IV) phosphate with a constant stirring, the resultant mixture were turned slowly into a greenish black colored slurries. The resultant slurries were kept for 24 hours at room temperature.

Now the poly-*o*-toluidine based composite cation-exchanger gels were filtered off, washed thoroughly with demineralized water (DMW) to remove excess acid and any adhering traces of potassium per sulphate. The washed gels were dried over P_4O_{10} at 30 °C in an oven. The dried products were immersed in DMW to obtain small granules. Samples were converted to the H^+ form by keeping in 1 M HNO_3 solution for 24 hours with occasionally shaking intermittently replacing the supernatant liquid. The excess acid was removed after several washing with DMW. The material was finally dried at 40 °C and sieving to obtain particles of particular size range (~125 μm). Hence a number of poly-*o*-toluidine Zr(IV) phosphate nanocomposite cation-exchanger samples were prepared and on the basis of Na^+ ion-exchange capacity (*i.e.c.*), percent of yield and physical appearance, sample S-5 (Table 1) was selected for further studies.

Table 1. Conditions of preparation and the ion-exchange capacity of poly-*o*-toluidine Zr(IV) phosphate nanocomposite cation-exchange materials

Sample	Mixing volume ratio						Appearance of beads after dyeing	Na^+ ion-exchange capacity in meq dry g^{-1}
	0.1 M $ZrOCl_2 \cdot 8H_2O$ in 4 M HCl	H_3PO_4 in DMW	pH of the inorganic precipitate	0.4M $(NH_4)_2S_2O_8$ in 2 M HCl	20% <i>o</i> -toluidine in 2 M HCl			
S-1	1	1(2 M)	1	-	-	White granular	0.34	
S-2	1	1(2 M)	2	-	-	White granular	1.46	
S-3	-	-	-	1	1	Greenish granular	0.7	
S-4	1	1(2M)	2	1	1	Greenish black	0.77	
S-5	1	2(3M)	2	1	1	Greenish black	1.71	
S-6	1	1.5(3M)	2	1	1	Greenish black	0.95	

Preparation of nylon-6,6 Sn (IV) phosphate composite cation-exchange material

Stannic(IV) phosphate precipitates were obtained by adding 0.10 mol dm^{-3} stannic chloride ($\text{SnCl}_4 \cdot 5\text{H}_2\text{O}$) solution prepared in 4.0 mol dm^{-3} HCl at the flow rate of $0.50 \text{ cm}^3 \text{ min}^{-1}$ to solutions of 0.10 mol dm^{-3} disodium hydrogen orthophosphate (Na_2HPO_4) solution prepared in DMW of different molarities. The white precipitates were obtained, when the pH of the mixtures was adjusted 1.0 by adding aqueous ammonia with constant stirring. The gels of nylon-6,6 prepared in concentrated formic acid were added into the white inorganic precipitate of Sn(IV) phosphate and mixed thoroughly with constant stirring. The white fibers were obtained which were kept for 24 h at room temperature for digestion. The supernatant liquid was decanted and fibers were filtered by suction. The excess acid was removed by several washings with DMW and the materials were dried in an air oven over P_4O_{10} at 40°C . The dried products were converted to H^+ -form by treating with 1.0 mol dm^{-3} HNO_3 for 24 h with occasional shaking intermittently replacing the supernatant liquid with fresh acid. The excess acid was removed after several washings with DMW and finally dried at 50°C . Hence, a number of samples of 'nylon-6,6 Sn(IV) phosphate' fibrous cation-exchanger were prepared (Table 2) and on the basis of Na^+ ion-exchange capacity (IEC), percentage of yield and physical appearance of material, sample P-4 was selected for detailed studies.

Table 2. Conditions of preparation and the ion-exchange capacity of Nylon-6,6, Sn(IV) phosphate composite cation-exchange material

Sample	Mixing volume ratio						Appearance of fiber after dyeing	Na^+ ion-exchange capacity in (m mol g^{-1})
	2.1 mol dm^{-3} $\text{SnCl}_4 \cdot 5\text{H}_2\text{O}$ in 4 mol dm^{-3} HCl	2.1 mol dm^{-3} Na_2HPO_4 in DMW	pH of the inorganic precipitate	Nylon-6,6 g	Formic acid. mL			
P-1	2	2	1	-	-	White granular	2.35	
P-2	0.5	1.5	1	1	10	White fiber	1.47	
P-3	1.5	1.5	1	2	10	White fiber	1.88	
P-4	2	2	1	1	10	White fiber	2.1	

Ion-exchange kinetics

The kinetic behavior of cation-exchange material for the exchange of various metal ions was studied on the composite cation-exchanger samples (S-5 and P-4) in the H^+ form.

Determination of infinite time of exchange

The infinite time of exchange is the time necessary to obtain equilibrium in an ion-exchange process. The ion-exchange rate becomes independent of time after this time interval as evident from Figure 1 and Figure 2. About 35 minutes for sample S-5 and 40 minute for sample P-4 were required for the establishment of equilibrium at 30°C for $\text{Mg}^{2+} - \text{H}^+$ exchange. Similar behaviors were observed for $\text{Ca}^{2+} - \text{H}^+$, $\text{Sr}^{2+} - \text{H}^+$, $\text{Ba}^{2+} - \text{H}^+$, $\text{Ni}^{2+} - \text{H}^+$, $\text{Cu}^{2+} - \text{H}^+$, $\text{Mn}^{2+} - \text{H}^+$ and $\text{Zn}^{2+} - \text{H}^+$, exchanges. Therefore 35 and 40 minutes have been assumed to be the infinite time of exchange for these studies.

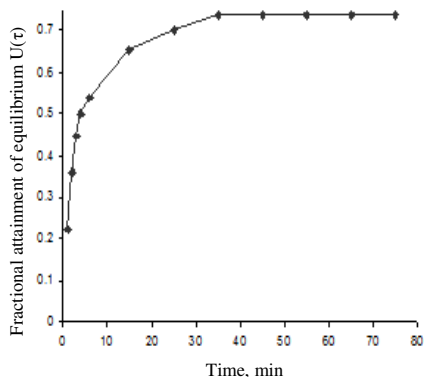


Figure 1. A plot of $U(\tau)$ vs. time for M(II)-H(I) exchanges at 30 °C on poly-*o*-toluidine Zr(IV) phosphate nanocomposite cation-exchanger for the determination of infinite time

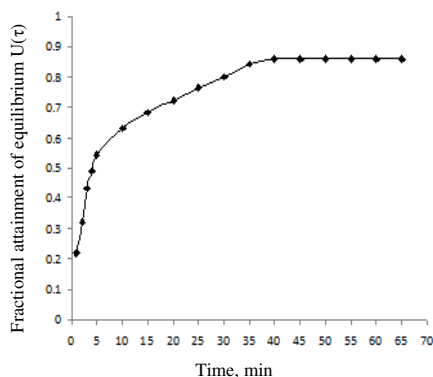


Figure 2. A plot of $U(\tau)$ vs. time for M(II)-H(I) exchanges at 30 °C on nylon-6,6 Sn(IV) phosphate composite cation-exchanger for the determination of infinite time

Kinetic measurements

The composite cation-exchange material samples (S-5 and P-4) were grounded and then sieved to obtain particles of definite mesh size (25-50, 50-70, 70-100 and 100-125). Out of them the particles of mean radii $\sim 125 \mu\text{m}$ (50-70 mesh) were selected to evaluate various kinetic parameters. The rate of exchange was determined by limited bath technique as follows:

Twenty milliliter fractions of the 0.03 M metal ion solutions (Mg, Ca, Sr, Ba, Ni, Cu, Mn and Zn) were shaken with 200 mg of the cation-exchangers in H^+ -form in several stoppered conical flasks at the desired temperatures for different time intervals (1.0, 2.0, 3.0, 4.0 and 5.0 min). The supernatant liquid was removed immediately and determinations were made, usually by EDTA titration²². Each set was repeated four times and the mean value was taken for calculations.

Analytical procedures

The results are expressed in terms of the fractional attainment of equilibrium, $U(\tau)$ with time according to the equation

$$U(\tau) = \frac{\text{the amount of exchange at time 't'}}{\text{the amount of exchange at infinite time}} \quad (1)$$

Results and Discussion

Various samples of a new and novel organic-inorganic composite cation-exchange material have been developed by the incorporation of polymer poly-*o*-toluidine and nylon-6,6 into the inorganic matrices of Zr(IV) phosphate and fibrous Sn(IV) phosphate. Due to high percentage of yield, better ion-exchange capacity, reproducible behavior, chemical and thermal stabilities samples S-5 and P-4 were chosen for detail ion-exchange studies. These composite cation-exchange materials possessed a better Na^+ ion-exchange capacity (1.71 meq g^{-1}) for POTZr(IV)P as compared to inorganic precipitate of Zr(IV) phosphate (0.34 meq g^{-1}) and (2.1 meq g^{-1}) for nylon 6,6 Sn(IV) phosphate as compared to Sn(IV) phosphate (2.35 meq g^{-1}).

*Ion-exchange kinetic studies on poly-*o*-toluidine Zr(IV) phosphate and nylon-6,6 Sn(IV) phosphate composite materials*

Kinetic measurements were made under conditions favoring a particle diffusion-controlled ion-exchange phenomenon for the exchange of Mg(II)–H(I), Ca(II)–H(I), Sr(II)–H(I), Ba(II)–H(I), Ni(II)–H(I), Cu(II)–H(I), Mn(II)–H(I) and Zn(II)–H(I). The particle diffusion controlled phenomenon is favored by a high metal ion concentration, a relatively large particle size of the exchanger and vigorous shaking of the exchanging mixture.

The infinite time of exchange is the time necessary to obtain equilibrium in an ion-exchange process. The ion-exchange rate becomes independent of time after this interval. Figure 1 and Figure 2 shows that 35 and 40 min were required for the establishment of equilibrium at 30 °C for Mg²⁺–H⁺ exchange for poly-*o*-toluidine Zr(IV) phosphate (S-5) and nylon-6,6 Sn(IV) phosphate (P-4) respectively. Similar behavior was observed for Ca²⁺–H⁺, Sr²⁺–H⁺, Ba²⁺–H⁺, Ni²⁺–H⁺, Cu²⁺–H⁺, Mn²⁺–H⁺ and Zn²⁺–H⁺ exchanges. Therefore, 35 min and 40 min were assumed to be the infinite time of exchange for the systems.

A study of the concentration effect on the rate of exchange at 30 °C showed that the initial rate of exchange was proportional to the metal ion concentration at and above 0.03 M for poly-*o*-toluidine Zr(IV) phosphate, S-5 (Figure 3) while 0.04 M for nylon-6,6 Sn(IV) phosphate, P-4 (Figure 4). Below the concentration of 0.02 M, film diffusion control was more prominent for the materials.

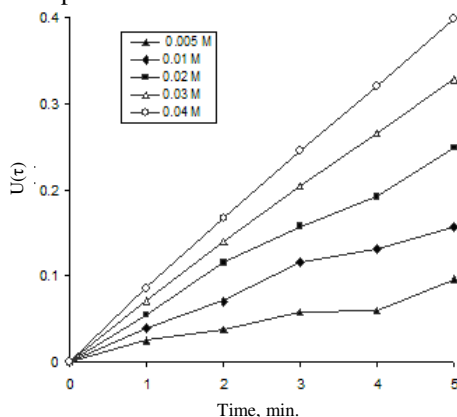


Figure 3. A plot of τ versus t (time) for M(II)-H(I) exchanges at 35 °C on a poly-*o*-toluidine Zr(IV) phosphate nanocomposite cation-exchanger using different solution concentration

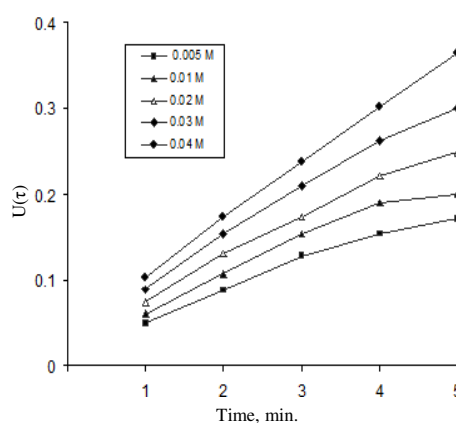


Figure 4. A plot of τ vs. t (time) for M(II)–H(I) exchanges at 45 °C on nylon-6,6 Sn(IV) phosphate composite cation-exchanger using different metal solution concentration

Plots of $U(\tau)$ versus t (min), for all metal ions (Figure 5 and Figure 6) indicated that the fractional attainment of equilibrium was faster at a higher temperature suggesting that the mobility of the ions increased with the increase in temperature and the uptake decreased with time. Each value of $U(\tau)$ will have a corresponding value of τ a dimensionless time parameter. On the basis of the Nernst-Planck equation, the numerical results can be expressed by explicit approximation²³⁻²⁵.

$$U(\tau) = \left\{ 1 - \exp \left[\pi^2 (f_1(\alpha) \tau + f_2(\alpha) \tau^2 + f_3(\alpha) \tau^3) \right] \right\}^{1/2} \quad (2)$$

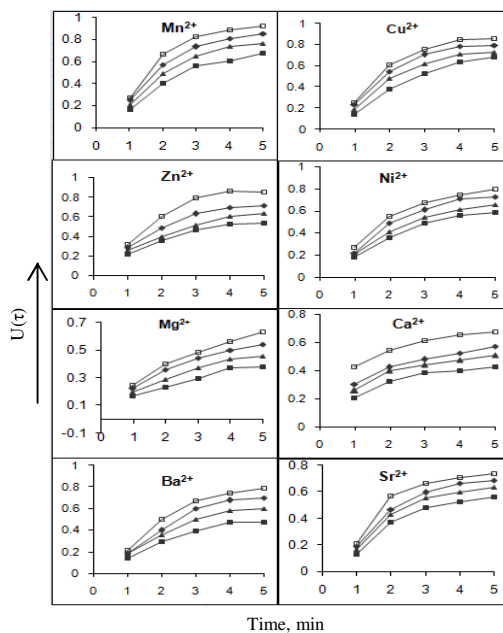


Figure 5. Plots of $U(\tau)$ versus t (Time) for different M(II)- H(I) exchanges at different temperature: (■) 30 °C; (▲) 45 °C; (◆) 60 °C; (□) 75 °C on poly-*o*-toluidine Zr(IV) phosphate nano-composite cation-exchanger

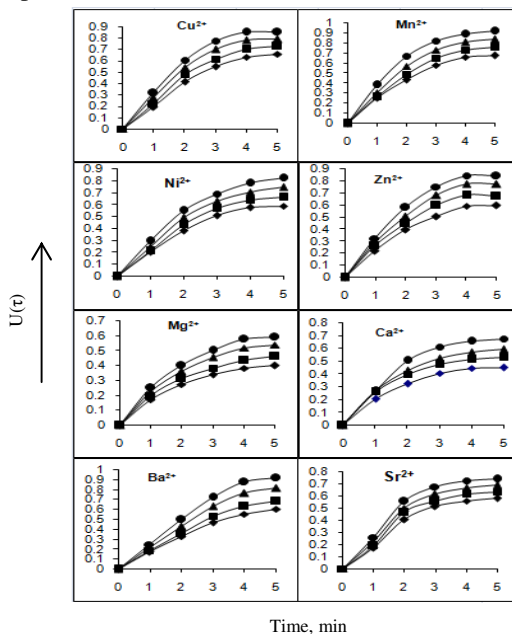


Figure 6. Plots of $U(\tau)$ vs. t (time) for different M(II)-H(I) exchanges at different temperature: (◆) 30 °C; (■) 45 °C; (▲) 60 °C; (●) 75 °C on nylon-6,6 Sn(IV) phosphate composite cation exchanger

Where τ is the half time of exchange $= \bar{D}_{H^+} t / r_0^2$, α is the mobility ratio $= \bar{D}_{H^+} / \bar{D}_{M^{2+}}$, r_0 is the particle radius, \bar{D}_{H^+} and $\bar{D}_{M^{2+}}$ are the inter diffusion coefficients of counter ions H^+ and M^{2+} respectively in the exchanger phase. The three functions $f_1(\alpha)$, $f_2(\alpha)$ and $f_3(\alpha)$, depend upon the mobility ratio (α) and the charge ratio ($Z_{H^+} / Z_{M^{2+}}$) of the exchanging ions. Thus they have different expressions as given below. When the exchanger is taken in the H^+ form and the exchanging ion is M^{2+} , for $1 \leq \alpha \leq 20$, as in the present case, the three functions have the values:

$$f_1(\alpha) = -\frac{1}{0.64 + 0.36\alpha^{0.668}}, \quad (3)$$

$$f_2(\alpha) = -\frac{1}{0.96 - 2.0\alpha^{0.4635}}, \quad (4)$$

$$f_3(\alpha) = -\frac{1}{0.27 + 0.09\alpha^{1.140}} \quad (5)$$

Each value of $U(\tau)$ will have a corresponding value of τ which is obtained on solving Eq. (ii) using a computer. The plots of τ versus time (t) at the four temperatures, as shown in Figure 7 and Figure 8, are straight lines passing through the origin, confirming the particle diffusion control phenomenon for M(II)–H(I) exchanges at a metal ion concentration of 0.03 M for poly-*o*-toluidine Zr(IV) phosphate (S-5) while 0.04 M for nylon-6,6 Sn(IV) phosphate. The slopes (S values) of various τ versus time (t) plots are given in Table 3 and Table 4.

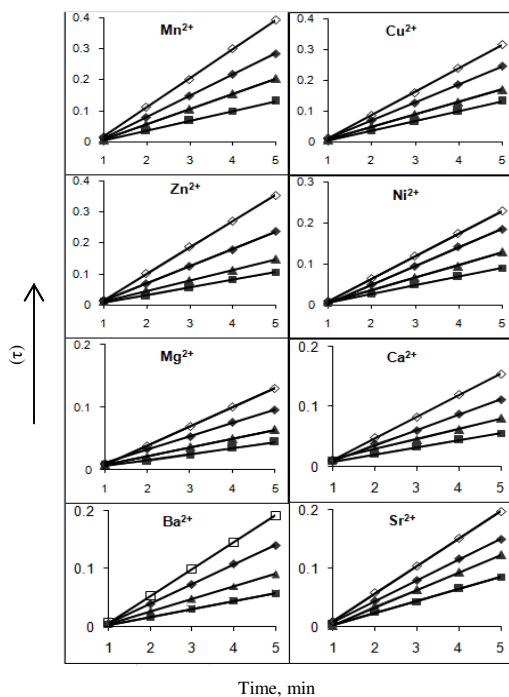


Figure 7. Plots of τ versus t (Time) for different M(II)–H(I) exchanges at different temperature: (■) 30 °C; (▲) 45 °C; (◆) 60 °C; (□) 75 °C on poly-*o*-toluidine Zr(IV) phosphate nanocomposite cation-exchanger

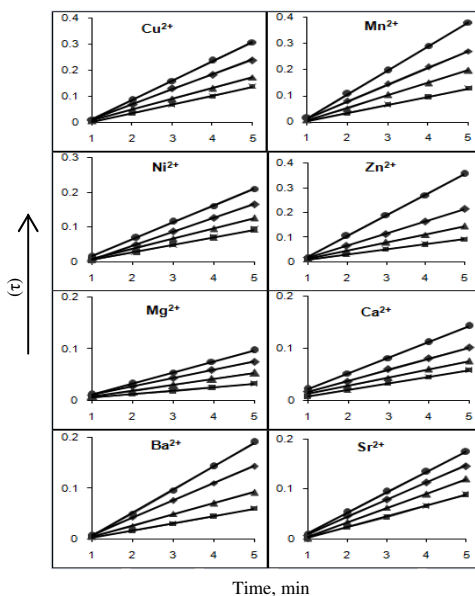


Figure 8. Plots of τ vs. t (time) for different M(II)–H(I) exchanges at different temperature: (■) 30 °C; (▲) 45 °C; (◆) 60 °C; (●) 75 °C on nylon-6,6 Sn(IV) phosphate-composite cation-exchanger

Table 3. Slopes of various τ versus time (t) plots on poly-*o*-toluidine Zr(IV) phosphate nanocomposite cation-exchanger at different temperatures

Migrating ions	$10^2 S, s^{-1}$			
	30 °C	45 °C	60 °C	75 °C
Mn(II)	3.1	4.9	6.7	9.2
Cu(II)	3.1	4.1	5.8	7.6
Ni(II)	2.1	3.0	4.5	5.4
Zn(II)	2.5	3.3	5.5	8.5
Mg(II)	0.9	1.4	2.1	3.0
Ca(II)	1.1	1.6	2.5	3.5
Ba(II)	1.3	2.1	3.3	4.6
Sr(II)	2.0	2.9	3.5	4.6

Table 4. Slopes of various τ versus time (t) plots on nylon-6,6 Sn(IV) phosphate composite cation-exchanger at different temperatures

Migrating ions	$10^2 S, s^{-1}$			
	30 °C	45 °C	60 °C	75 °C
Mn(II)	3.0	4.8	6.4	9.1
Cu(II)	3.3	4.1	5.7	7.4
Ni(II)	2.1	2.9	4.0	4.8
Zn(II)	2.0	3.2	4.9	8.4
Mg(II)	0.6	1.1	1.6	2.1
Ca(II)	1.2	1.5	2.1	3.0
Ba(II)	1.4	2.1	3.4	4.5
Sr(II)	2.1	2.9	3.4	4.1

The S values are related to \bar{D}_{H^+} as follows:

$$S = \bar{D}_{H^+} / r_0^2, \quad (6)$$

The values of $-\log \bar{D}_{H^+}$ obtained by using Eq. (6) plotted against $1000/T(K)$ are straight lines as shown in Figure 9 and Figure 10, thus verifying the validity of the Arrhenius relation;

$$\log \bar{D}_{H^+} = D_0 \exp(-E_a / RT) \quad (7)$$

D_0 is obtained by extrapolating these lines and using the intercepts at the origin. The activation energy (E_a) is then calculated with the help of the Eq.(7), putting the value of \bar{D}_{H^+} at 273 K. The entropy of activation (ΔS°) were then calculated by substituting D_0 in Eq. (8).

$$D^\circ = 2.72d^2 (kT/h) \exp(\Delta S^\circ / R) \quad (8)$$

Where d is the ionic jump distance taken as 5 \AA , k is the Boltzmann²⁶ constant, R is the gas constant, h is Plank's constant and T is taken as 273 K. The values of the diffusion coefficient (D_0), energy of activation (E_a) and entropy of activation (ΔS°), thus obtained are summarized in Table 5 and Table 6.

The kinetic study reveals that equilibrium is attained faster at a higher temperature (Figure 7 and Figure 8), probably because of a higher diffusion rate of ions through the thermally enlarged interstitial positions of the ion-exchange matrix. The particle diffusion phenomenon is evident from the straight lines passing through the origin for the τ versus time (t) plots, as shown in Figure 9 and Figure 10. Negative values of the entropy of activation suggest a greater degree of order achieved during the forward ion-exchange in M(II)–H(I) process. From the Table 5 and Table 6, it is observed that the self-diffusion co-efficient is highest for Ba^{2+} ion. As ionic radii of Ba^{2+} ion is greater, the Ba^{2+} ion is least hydrated and therefore its self-diffusion co-efficient is higher.

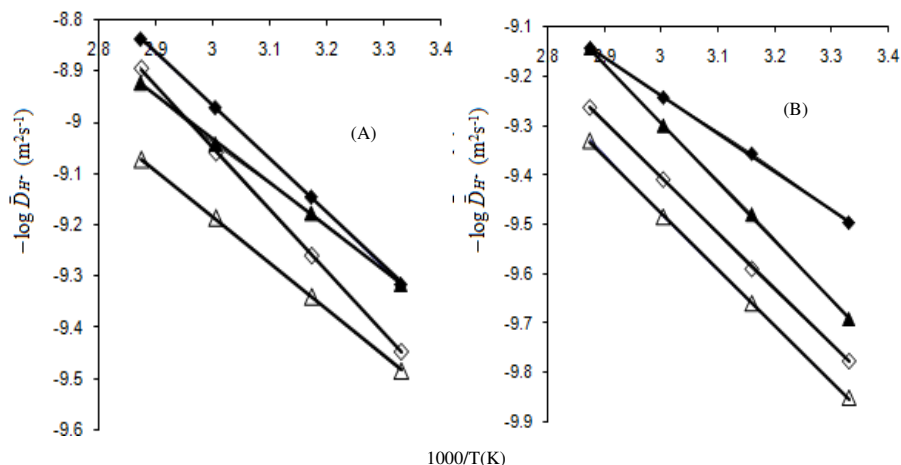


Figure 9. Plots of $-\log \bar{D}_{H^+}$ vs. $1000/T$ (K) for (A): (■) Mn(II); (▲) Cu(II); (Δ) Ni(II); (□) Zn(II), and (B): (Δ) Mg(II); (□) Ca(II); (▲) Ba(II); (■) Sr(II) on poly-*o*-toluidine Zr(IV) phosphate nanocomposite cation-exchanger

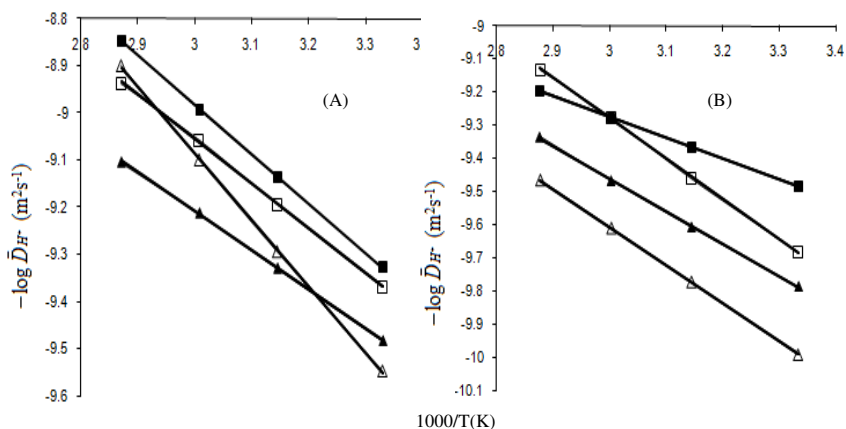


Figure 10. Plots of $-\log \bar{D}_{H^+}$ vs. $1000/T$ (K) for (A): (■) Mn(II); (□) Cu(II); (▲) Ni(II); (Δ) Zn(II) and (B): (Δ) Mg(II); (▲) Ca(II); (□) Ba(II); (■) Sr(II) on nylon-6,6 Sn(IV) phosphate composite cation-exchanger

Table 5. Values of D_0 , E_a and ΔS^0 for the exchange of H(I) with some metal ions on poly-*o*-toluidine Zr(IV) phosphate nanocomposite cation-exchanger

Metal ion exchange with H(I)	10^9 Ionic mobility, $m^2 V^{-1} s^{-1}$	10^2 ionic Radii, nm	$10^7 D_0$, $m^2 s^{-1}$	E_a , $10^2 k J mol^{-1}$	ΔS^0 , $J K^{-1} mol^{-1}$
Mn(II)	55	9.1	14.75	104.54	0.05
Cu(II)	57	7.0	3.24	84.83	0.16
Ni(II)	52	7.8	3.29	90.09	0.15
Zn(II)	56	8.3	37.03	120.57	0.90
Mg(II)	55	7.8	9.02	114.40	0.29
Ca(II)	62	10.6	9.66	113.01	0.32
Ba(II)	62	12.7	20.11	119.91	0.64
Sr(II)	66	14.3	1.20	77.22	0.59

Table 6. Values of D_0 , E_a and ΔS^0 for the exchange of H(I) with some metal ions on nylon-6,6 Sn(IV) phosphate composite cation-exchanger

Metal ion exchange with H(I)	10^9 Ionic mobility, $m^2 V^{-1} s^{-1}$	10^2 ionic radii, nm	$10^7 D_0$, $m^2 s^{-1}$	E_a , $10^2 k J mol^{-1}$	ΔS^0 , $J K^{-1} mol^{-1}$
Mn(II)	55	9.1	14.56	104.9	0.50
Cu(II)	57	7.0	6.28	95.1	0.13
Ni(II)	52	7.8	1.89	82.9	0.39
Zn(II)	56	8.3	142.5	141.3	1.49
Mg(II)	55	7.8	6.78	114.6	0.16
Ca(II)	62	10.6	3.08	98.3	0.18
Ba(II)	62	12.7	23.53	121.6	0.70
Sr(II)	66	14.3	0.43	63.5	1.04

Conclusion

Poly-*o*-toluidine Zr(IV) phosphate, a nonocomposite cation-exchange material, having excellent ion-exchange capacity (1.71 meq g^{-1}) as compared to inorganic precipitate of Zr(IV) phosphate (0.34 meq g^{-1}) and (2.1 meq g^{-1}) for nylon 6,6 Sn(IV) phosphate, a fibrous cation-exchange material as compared to Sn(IV) phosphate (2.35 meq g^{-1}) have been synthesized by sol gel method and taken for detailed ion exchange studies. Linear τ (dimensionless time parameter) vs. t (time) plots suggests the particle diffusion mechanism of ion exchange. Further, various kinetic parameters like self-diffusion coefficient (D_0), Energy of activation (E_a) and entropies of activation (ΔS°) have been evaluated under condition favoring a particle diffusion-controlled mechanism. Nylon-6,6 Sn(IV) phosphate shows better cation-exchange kinetic studies than poly-*o*-toluidine Zr(IV) phosphate.

Acknowledgement

The authors are thankful to Department of Applied Chemistry, Z.H. College of Engineering and Technology, A.M.U., (Aligarh) for providing research facilities. Assistance provided by the, I.I.T. Delhi, AIIMS Delhi and I.I.T. Roorkee to carry out some instrumental analysis.

References

1. Samsonov G V, Trostyanskaya E B and El'kin G E, Ion Exchange, sorbtion of Organic Substances; Nauk, Leningrad: 1969, 282.
2. Inglezakis V, Pouloupoulos S, Adsorption, Ion-exchange and catalysis: Design of operations and environmental applications, 1st Ed., U K, 2006
3. Andrei A Zagorodni, Ion exchange materials: Properties and applications: 1st Ed., U K, 2007.
4. Olive H and Lacoste G, *Electrochimica Acta*, 1980, **25**, 1303-1308.
5. Kusumoto I, *J Nutr.*, 2001, **131(9)**, 2552S-2555S.
6. Sherman J D, *Sci Tech.*, 1984, **80**, 583-623.
7. Dale J A, Nikitin N V, Moore R, Opperman D, Crooks J, Naden D, Belsten E and Jenkins P; In Ion Exchange at The Millanium (Greig J A, Ed.) Imperial College Press: London, 2000, 261.
8. Shahidi F, Arachchi J K V and You-Jin Jeon, *Trends in Food Sci Tech.*, 1999, **10**, 37-51.
9. Das K, Anis M, Azemi B M N M and Ismail N, *Biotechnol Bioeng.*, 1995, **48(5)**, 551-555.
10. Fuh W S and Chiang B H, *J Food Sci.*, 1990, **55(5)**, 1454-1457.
11. Calle E V, Ruales J, Dornier M, Sandeaux J, Sandeaux R and Pourcelly G *Desalination*, 2002, **149**, 357.
12. Vera E, Ruales J, Dornier M, Sandeaux J, Persin F, Porcelly G, Vaillant F and Reynes M, *J Food Eng.*, 2003, **59(4)**, 361-367.
13. Murai Y, Yamadera T and Koike Y, *Desalination*, 1977, **23**, 97-104.
14. Kentish S E and Stevens G W, *Chem Engg J.*, 2001, **84(2)**, 149-159.
15. Nakanishi T, Higuchi N, Nomura M, Aida M and Fujii; m Y, *J Nucl Sci Technol.*, 1996, **33**, 341-345.
16. Harjula R, Lehto J, Paajanen A, Brodtkin L and Tusa E, *Nucl Sci Engg.*, 2001, **137**, 206.
17. Harjula R, Lehto J, Paajanen A, Tusa E and Yarnel P, *React Funct Polym.*, 2004, **60**, 85-95.
18. Bolto B A, Swenton E A, Nadebaum P R and Murtagh R W, *Water Sci Tech.*, 1982, **14**, 523.
19. Mulder M, Basic Principles of Membrane Technology, Kluwer Academic Publishers: Dordrecht, 1982.

20. Mavrov V, Chmiel H, Heitele B and Rogener F, *Desalination*, 1997, **108(1-3)**, 159-166.
21. Zagorodni A A, *Ion Exchange Materials: Properties and Applications*, Elsevier, Amsterdam, 2006.
22. Reilly C N, Schmidt R W and Sadek F S, *J Chem Edu.*, 1959, **36(11)**, 555.
23. Vermeulen T, *Ind Eng Chem.*, 1953, **45**, 1664.
24. Helfferich F and Plesset M S, *J Chem Phys.*, 1958, **28**, 418.
25. Plesset M S, Helfferich F and Franklin J N, *J Chem Phys.*, 1958, **29**, 1064.
26. Barrer R M, Bertholomew R F and Rees L V C, *Phys Chem Solids*, 1961, **21**, 12.